

WCAP-10586

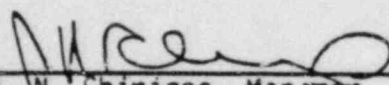
TECHNICAL BASES FOR ELIMINATING LARGE
PRIMARY LOOP PIPE RUPTURE AS A STRUCTURAL
DESIGN BASIS FOR MILLSTONE UNIT 3

JUNE 1984

E. L. Furchi
H. F. Clark, Jr.

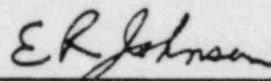
S. A. Swamy
R. A. Holmes

APPROVED:



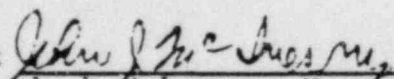
J. W. Chirigos, Manager
Structural Materials Engineering

APPROVED:



E. R. Jonnson, Manager
Structural and Seismic
Development

APPROVED:



J. J. McInerney, Manager
Mechanical Equipment and Systems
Licensing

Work Performed under Shop Order NEUJ 950

WESTINGHOUSE ELECTRIC CORPORATION
NUCLEAR ENERGY SYSTEMS
P.O. Box 355
Pittsburgh, Pennsylvania 15230

FOREWORD

This document contains Westinghouse Electric Corporation proprietary information and data which has been identified by brackets. Coding associated with the brackets set forth the basis on which the information is considered proprietary. These codes are listed with their meanings in WCAP-7211.

The proprietary information and data contained in this report were obtained at considerable Westinghouse expense and its release could seriously affect our competitive position. This information is to be withheld from public disclosure in accordance with the Rules of Practice, 10 CFR 2.790 and the information presented herein be safeguarded in accordance with 10 CFR 2.903. Withholding of this information does not adversely affect the public interest.

This information has been provided for your internal use only and should not be released to persons or organizations outside the Directorate of Regulation and the ACRS without the express written approval of Westinghouse Electric Corporation. Should it become necessary to release this information to such persons as part of the review procedure, please contact Westinghouse Electric Corporation, which will make the necessary arrangements required to protect the Corporation's proprietary interests.

The proprietary information is deleted in the unclassified version of this report.

TABLE OF CONTENTS

<u>Section</u>	<u>Title</u>	<u>Page</u>
1.0	INTRODUCTION	1-1
1.1	Purpose	1-1
1.2	Scope	1-1
1.3	Objectives	1-1
1.4	Background Information	1-2
2.0	OPERATION AND STABILITY OF THE REACTOR COOLANT SYSTEM	2-1
2.1	Stress Corrosion Cracking	2-1
2.2	Water Hammer	2-2
2.3	Low Cycle and High Cycle Fatigue	2-3
3.0	PIPE GEOMETRY AND LOADING	3-1
4.0	FRACTURE MECHANICS EVALUATION	4-1
4.1	Global Failure Mechanism	4-1
4.2	Local Failure Mechanism	4-2
4.3	Material Properties	4-3
4.4	Results of Crack Stability Evaluation	4-4
5.0	LEAK RATE PREDICTIONS	5-1
6.0	FATIGUE CRACK GROWTH ANALYSIS	6-1
7.0	ASSESSMENT OF MARGINS	7-1
8.0	CONCLUSIONS	8-1
9.0	REFERENCES	9-1
APPENDIX A-	[a,c,e]	A-1

LIST OF TABLES

<u>Table</u>	<u>Title</u>	<u>Page</u>
3-1	Millstone Unit 3 Primary Loop Data	3-3
4-1	Chemical and Physical Properties of Millstone Unit No. 3 Primary Loop Material	4-6
6-1	Fatigue Crack Growth at [] ^{a,c,e}	6-3

LIST OF FIGURES

<u>Figure</u>	<u>Title</u>	<u>Page</u>
3-1	Schematic Diagram of Primary Loop Showing Weld Locations Millstone Unit 3	3-4
3-2	Reactor Coolant Pipe	3-5
4-1	[] ^{a,c,e} Stress Distribution	4-7
4-2	J- Δa Curves at Different Temperatures, Aged Material [] ^{a,c,e} (7500 Hours at 400°C)	4-8
4-3	Critical Flaw Size Prediction	4-9
6-1	Typical Cross-Section of [] ^{a,c,e}	6-4
6-2	Reference Fatigue Crack Growth Curves for [] ^{a,c,e}	6-5
6-3	Reference Fatigue Crack Growth Law for [] ^{a,c,e} in a Water Environment at 600°F	6-6
A-1	Pipe with a Through-Wall Crack in Bending	A-2

1.0 INTRODUCTION

1.1 Purpose

This report applies to the Millstone Unit 3 plant reactor coolant system primary loop piping. It is intended to demonstrate that specific parameters for the Millstone plant are enveloped by the generic analysis performed by Westinghouse in WCAP-9558, Revision 2 (Reference 1) (i.e., the reference report) and accepted by the NRC (Reference 2).

1.2 Scope

The current structural design basis for the Reactor Coolant System (RCS) primary loop requires that pipe breaks be postulated as defined in the approved Westinghouse Topical Report WCAP-8082 (Reference 3). In addition, protective measures for the dynamic effects associated with RCS primary loop pipe breaks have been incorporated in the Millstone plant design. However, Westinghouse has demonstrated on a generic basis that RCS primary loop pipe breaks are highly unlikely and should not be included in the structural design basis of Westinghouse plants (see Reference 4). In order to demonstrate the applicability of the generic evaluations to the Millstone plant, Westinghouse has performed a comparison of the Millstone plant loads and geometry with the envelope parameters used in the generic analyses (Reference 1), a fracture mechanics evaluation, a determination of leak rates from through wall cracks, a fatigue crack growth evaluation, and an assessment of margins.

1.3 Objectives

The conclusions of WCAP-9558, Revision 2 (Reference 1) support the elimination of RCS primary loop pipe breaks for Millstone Unit 3. In order to validate this conclusion the following objectives must be achieved.

- a. Demonstrate that the Millstone plant parameters are enveloped by generic Westinghouse studies.

- b. Demonstrate that margin exists between the critical crack size and a postulated crack which yields a detectable leak rate.
- c. Demonstrate that there is sufficient margin between the leakage through a postulated crack and the leak detection capability of the Millstone plant.
- d. Demonstrate that fatigue crack growth is negligible.

1.4 Background Information

Westinghouse has performed considerable testing and analysis to demonstrate that RCS primary loop pipe breaks can be eliminated from the structural design basis of all Westinghouse plants. The concept of eliminating pipe breaks in the RCS primary loop was first presented to the NRC in 1978 in WCAP-9283 (Reference 5). That Topical Report employed a deterministic fracture mechanics evaluation and a probabilistic analysis to support the elimination of RCS primary loop pipe breaks. This approach was then used as a means of addressing Generic Issue A-2 and Asymmetric LOCA Loads.

Westinghouse performed additional tests and analyses to justify the elimination of RCS primary loop pipe breaks. As a result of this effort, WCAP-9558, Revision 2, WCAP-9787, and Letter Report NS-EPR-2519 (References 1, 6, and 7) were submitted to the NRC.

The NRC funded research through Lawrence Livermore National Laboratory (LLNL) to address this same issue using a probabilistic approach. As part of the LLNL research effort, Westinghouse performed extensive evaluations of specific plant loads, material properties, transients, and system geometries to demonstrate that the analysis and testing previously performed by Westinghouse and the research performed by LLNL applied to all Westinghouse plants including Millstone (References 8 and 9). The results from the LLNL study were released at a March 28, 1983 ACRS Subcommittee meeting. These studies, which are applicable to all Westinghouse plants east of the Rocky Mountains, determined the mean probability of a direct LOCA (RCS primary loop pipe break) to be 10^{-10} per reactor year and the mean probability of an indirect LOCA to

be 10^{-7} per reactor year. Thus, the results previously obtained by Westinghouse (Reference 5) were confirmed by an independent NRC research study.

Based on the studies by Westinghouse, LLNL, the ACRS, and the AIF, the NRC completed a safety review of the Westinghouse reports submitted to address asymmetric blowdown loads that result from a number of discrete break locations on the PWR primary systems. The NRC Staff evaluation (Reference 2) concludes that an acceptable technical basis has been provided so that asymmetric blowdown loads need not be considered for those plants that can demonstrate the applicability of the modeling and conclusions contained in the Westinghouse response or can provide an equivalent fracture mechanics demonstration of the primary coolant loop integrity.

This report will demonstrate the applicability of the Westinghouse generic evaluations to Millstone Unit 3.

2.0 OPERATION AND STABILITY OF THE REACTOR COOLANT SYSTEM

The Westinghouse reactor coolant system primary loop has an operating history that demonstrates the inherent stability characteristics of the design. This includes a low susceptibility to cracking failure from the effects of corrosion (e.g., intergranular stress corrosion cracking), water hammer, or fatigue (low and high cycle). This operating history totals over 400 reactor-years, including five plants each having 15 years of operation and 15 other plants each with over 10 years of operation.

2.1 Stress Corrosion Cracking

For the Westinghouse plants, there is no history of cracking failure in the reactor coolant system loop piping. For stress corrosion cracking (SCC) to occur in piping, the following three conditions must exist simultaneously: high tensile stresses, a susceptible material, and a corrosive environment (Reference 10). Since some residual stresses and some degree of material susceptibility exist in any stainless steel piping, the potential for stress corrosion is minimized by properly selecting a material immune to SCC as well as preventing the occurrence of a corrosive environment. The material specifications consider compatibility with the system's operating environment (both internal and external) as well as other materials in the system, applicable ASME Code rules, fracture toughness, welding, fabrication, and processing.

The environments known to increase the susceptibility of austenitic stainless steel to stress corrosion are (Reference 10): oxygen, fluorides, chlorides, hydroxides, hydrogen peroxide, and reduced forms of sulfur (e.g., sulfides, sulfites, and thionates). Strict pipe cleaning standards prior to operation and careful control of water chemistry during plant operation are used to prevent the occurrence of a corrosive environment. Prior to being put into service, the piping is cleaned internally and externally. External cleaning for Class 1 stainless steel piping includes patch tests to monitor and control chloride and fluoride levels. During flushes and preoperational testing, water chemistry is controlled in accordance with written specifications.

Requirements on chlorides, fluorides, conductivity, and pH are included in the acceptance criteria for the piping.

During plant operation, the reactor coolant water chemistry is monitored and maintained within very specific limits. Contaminant concentrations are kept below the thresholds known to be conducive to stress corrosion cracking with the major water chemistry control standards being included in the plant operating procedures as a condition for plant operation. For example, during normal power operation, oxygen concentration in the RCS is expected to be less than 0.005 ppm by controlling charging flow chemistry and maintaining hydrogen in the reactor coolant at specified concentrations. Halogen concentrations are also stringently controlled by maintaining concentrations of chlorides and fluorides within the specified limits. This is assured by controlling charging flow chemistry and specifying proper wetted surface materials.

2.2 Water Hammer

Overall, there is a low potential for water hammer in the RCS since its design and operation precludes the voiding condition in normally filled lines. The reactor coolant system, including piping and primary components, is designed for normal, upset, emergency, and faulted condition transients. The design requirements are conservative relative to both the number of transients and their severity. Relief valve actuation and the associated hydraulic transients following valve opening are considered in the system design. Other valve and pump actuations result in relatively slow transients with no significant affect on the system's dynamic loads. To ensure dynamic system stability, reactor coolant parameters are stringently controlled. Temperature during normal operation is maintained within a narrow range by control rod position; pressure is controlled by pressurizer heaters and pressurizer spray also within a narrow range for steady-state conditions. The flow characteristics of the system remain constant during a fuel cycle because the only governing parameters namely system resistance and the reactor coolant pump characteristics are controlled in the design process. Additionally, Westinghouse has instrumented typical reactor coolant systems to verify the flow and vibration characteristics of the system. Preoperational testing and

operating experience have verified the Westinghouse approach. The operating transients of the RCS primary piping are such that no significant water hammer can occur.

2.3 Low Cycle and High Cycle Fatigue

Low cycle fatigue considerations are taken into account in the design of the piping system through the fatigue usage factor evaluation to show compliance with the rules of Section III of the ASME Code. A further evaluation of the low cycle fatigue loadings was carried out as part of this study in the form of a fatigue crack growth analysis, as discussed in Section 6.

High cycle fatigue loads in the system would result primarily from pump vibrations. These are minimized by restrictions placed on shaft vibrations during hot functional testing and operation. During operation, an alarm signals the exceedance of the vibration limits. Field measurements have been made on a number of plants during hot functional testing, including plants similar to Millstone. Stresses in the elbow region below the reactor coolant pump have been found to be very small, between 2 and 3 ksi at the highest. These stresses are well below the fatigue endurance limit for the material and would also result in an applied stress intensity factor below the threshold for fatigue crack growth.

3.0 PIPE GEOMETRY AND LOADING

The loop weld locations for Millstone are identified in Figure 3-1. The material properties and the loads at these locations resulting from deadweight, thermal expansion, and Safe Shutdown Earthquake (SSE) are provided in Table 3-1. The primary loop material is cast type SA-351-CF8A. As seen from this table, the junction of the hot leg and the reactor vessel outlet nozzle (Location 1) is the most limiting location for crack stability analysis based on the highest stress due to the combined pressure, deadweight, thermal expansion, and SSE loadings. A segment of the primary coolant hot leg pipe is sketched in Figure 3-2. This segment is postulated to contain a circumferential through-wall flaw. This location will be referred to as the critical location. The inside diameter and the wall thickness of the pipe are 29.2 and 2.37 inches, respectively. At this location, the axial force (F_x) and the bending moment (M_b) are []^{a,c,e} (including the axial force due to pressure) and []^{a,c,e} respectively. The pipe is subjected to a normal operating pressure of []^{a,c,e}. The method for calculating the loads found in Table 3-1 is described below.

The axial force F and transverse bending moments, M_y and M_z , are chosen for each static load (pressure, deadweight and thermal) based on elastic-static analyses for each of these load cases. These pipe load components are combined algebraically to define the equivalent pipe static loads F_s , M_{ys} , and M_{zs} . Based on elastic SSE response spectra analyses, amplified pipe seismic loads, F_d , M_{yd} , M_{zd} are obtained. The maximum pipe loads are obtained by combining the static and dynamic load components as follows:

$$F_x = |F_s| + |F_d|$$

$$M_b = \sqrt{M_y^2 + M_z^2}$$

where:

$$M_y = |M_{ys}| + |M_{yd}|$$

$$M_z = |M_{zs}| + |M_{zd}|$$

The corresponding geometry and loads used in the reference report (Reference 1) are as follows: inside diameter and wall thickness are 29.0 and 2.5 inches; axial load and bending moment are [

] ^{a,c,e} The outer fiber stress for Millstone is [] ^{a,c,e} while in the reference report it is [] ^{a,c,e} This demonstrates conservatism in the reference report which makes it more severe than the Millstone analyses.

The normal operating loads (i.e., algebraic sum of pressure, deadweight, and 100 percent power thermal expansion loading) at the critical location, i.e., the junction of the hot leg and the reactor vessel outlet nozzle, are as follows:

$$F = []^{a,c,e} \text{ (including internal pressure)}$$

$$M = []^{a,c,e}$$

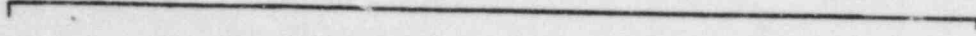
The calculated and allowable stresses for ASME Code Section III, NB-3600 equation 9 (faulted, i.e., pressure, deadweight, and SSE) and equation 12 (thermal) at the critical location are as follows:

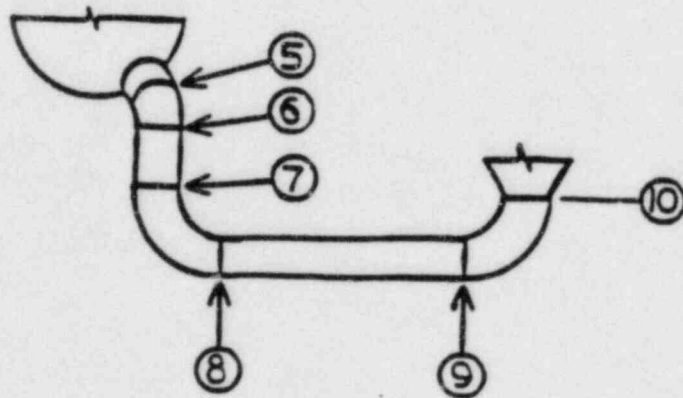
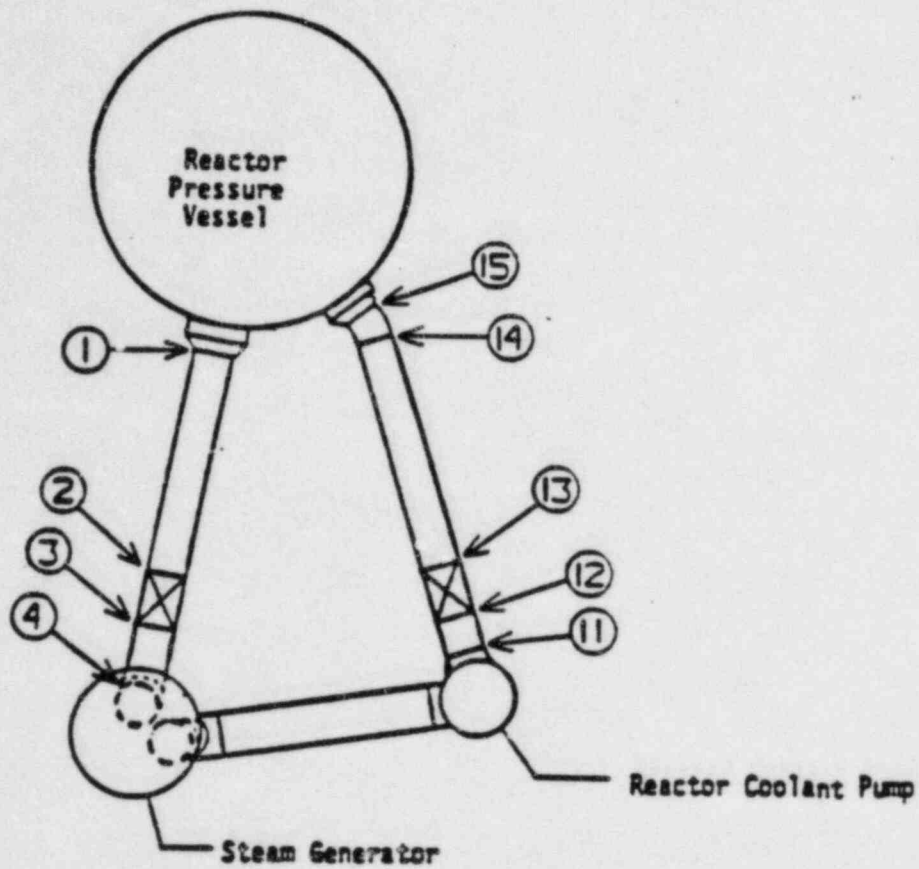
<u>Equation Number</u>	<u>Calculated Stress (ksi)</u>	<u>Allowable Stress (ksi)</u>	<u>Ratio of Calculated/Allowable</u>
[]

TABLE 3-1

MILLSTONE UNIT #3 PLANT PRIMARY LOOP DATA

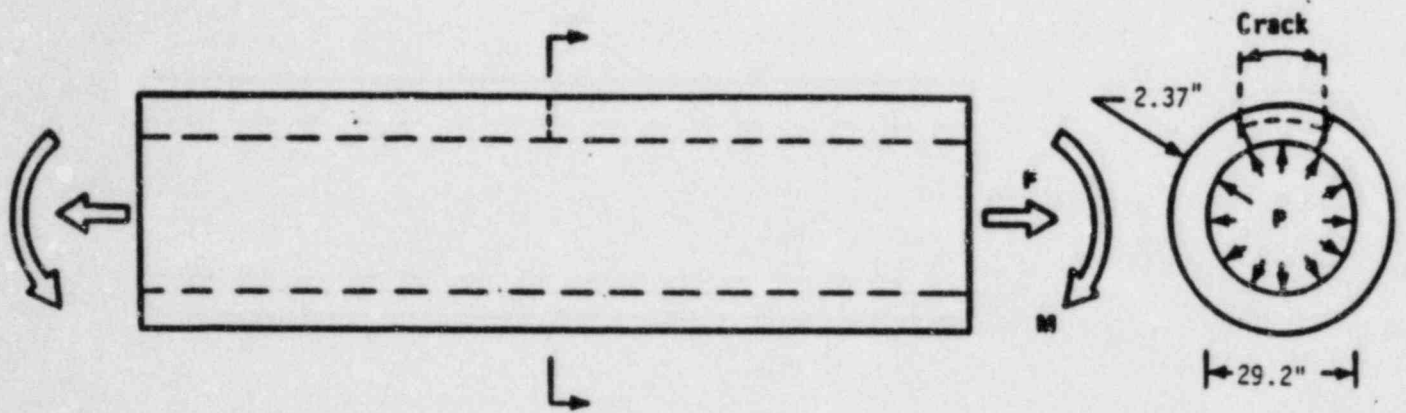
a,c,e





a, c, e

FIGURE 3-1 Schematic Diagram of Primary Loop Showing Weld Locations - Millstone Unit 3



[a,c,e]

FIGURE 3-2 Reactor Coolant Pipe

4.0 FRACTURE MECHANICS EVALUATION

4.1 Global Failure Mechanism

Determination of the conditions that lead to failure in stainless steel must be done with plastic fracture mechanics methods because of the large amount of deformation accompanying fracture. A conservative method for predicting the failure of ductile material is the [

] ^{a,c,e} This methodology has been shown through a large number of experiments to be applicable to ductile piping and will be used here to predict the critical flaw size in the primary coolant piping. The failure criterion has been obtained by requiring [

] ^{a,c,e} (Figure 4-1) when loads are applied. The detailed development is provided in Appendix A for a through-wall circumferential flaw in a pipe with internal pressure, axial force, and imposed bending moments. The [^{a,c,e} for such a pipe is given by:

[] ^{a,c,e}

where:

[] ^{a,c,e}

[

]

a,c,e

The analytical model described above accurately accounts for the piping internal pressure as well as the imposed axial force as they affect []^{a,c,e} Good agreement was found between the analytical predictions and the experimental results (Reference 11).

4.2 Local Failure Mechanism

The local mechanism of failure is primarily dominated by the crack tip behavior in terms of crack-tip blunting, initiation, extension, and finally crack instability. Depending on the material properties and geometry of the pipe, flaw size, shape and loading, the local failure mechanisms may or may not govern the ultimate failure.

The stability will be assumed if the crack does not initiate at all. It has been accepted that the initiation toughness measured in terms of J_{IN} (i.e., J_{IC})^a from a J-integral resistance curve is a material parameter defining the crack initiation. If, for a given load, the calculated J-integral value is shown to be less than J_{IN} of the material, then the crack will not initiate. If the initiation criterion is not met, one can calculate the tearing modulus as defined by the following relation:

^a The notation J_{IN} instead of J_{IC} was used in Reference 1 to designate the value of the J-integral at crack initiation; the J_{IN} notation will be used in this report in keeping with Reference 1.

$$T_{app} = \frac{dJ}{da} \frac{E}{\sigma_f^2}$$

where:

T_{app} = applied tearing modulus

E = modulus of elasticity

$\sigma_f = [\quad]^{a,c,e}$ (flow stress)

a = crack length

[]^{a,c,e}

In summary, the local crack stability will be established by the two-step criteria:

$$J < J_{IN}$$

$$T_{app} < T_{mat}, \text{ if } J \geq J_{IN}$$

4.3 Material Properties

The material in the Millstone Unit 3 primary loop and associated welds is cast stainless steel (SA-351-CF8A). The tensile and flow properties at the critical location, the hot leg and the reactor vessel outlet nozzle junction, are given in Table 3-1.

The fracture properties of CF8A cast stainless steel have been determined through fracture tests carried out at 600°F and reported in Reference 12. This reference shows that J_{IN} for the base metal ranges from [$\quad]^{a,c,e}$ for the multiple tests carried out.

Cast stainless steels are subject to thermal aging during service. This thermal aging causes an elevation in the yield strength of the material and a degradation of the fracture toughness, the degree of degradation being proportional to the level of ferrite in the material. To determine the effects of thermal aging on piping integrity, a detailed study was carried out

in Reference 13. In that report, fracture toughness results were presented for a material representative of [

] ^{a,c,e} Toughness results were provided for the material in the fully aged condition and these properties are also presented in Figure 4-2 of this report. The J_{IN} value for this material at operating temperature was approximately [] ^{a,c,e} and the maximum value of J obtained in the tests was in excess of [] ^{a,c,e}. The tests for this material were conducted on small specimens and therefore rather short crack extensions resulted. (Maximum extension was 4.3 mm.) Therefore it is expected that higher J values would be sustained for larger specimens. The effect of the aging process on loop piping integrity for Millstone is addressed in Table 4-1, where the plant specific material chemistry for the loop materials is considered. This table shows that the degree of thermal aging expected by end-of-life is less than that produced in [] ^{a,c,e}. Therefore the J_{IN} values for the Millstone Unit 3 at end-of-life would be expected to be considerably higher than those reported for [] ^{a,c,e} in Figure 4-2 (also see Reference 14). In addition, the tearing modulus for the Millstone Unit 3 material would be greater than [] ^{a,c,e}.

Available data on stainless steel welds indicate that the J_{IN} values for the worst case welds are on the same order as the aged material, but the slope of the J-R curve is steeper, and higher J-values have been obtained from fracture tests (in excess of 3000 in-lbs/in²). The applied value of the J-integral for a flaw in the weld regions will be lower than that in the base metal because the yield stress for the weld materials is much higher at the operating temperature. Therefore, weld regions are less limiting than the cast material.

4.4 Results of Crack Stability Evaluation

Figure 4-3 shows a plot of the [] ^{a,c,e} as a function of through-wall circumferential flaw length in the [] ^{a,c,e} of the main coolant piping. This [] ^{a,c,e} was calculated for Millstone using data for a pressurized pipe at [] ^{a,c,e} properties.

The maximum applied bending moment of []^{a,c,e} can be plotted on this figure, and used to determine a critical flaw length, which is shown to be []^{a,c,e}. This is considerably larger than the []^{a,c,e} reference flaw used in Reference 1.

[

[]^{a,c,e} The axial load used in the present case is 13 percent higher than that used in Reference 1. However, the []^{a,c,e} percent of the moment load used in Reference 1. The maximum outer fiber stress for Millstone is only 78 percent of that of Reference 1. [

[]^{a,c,e} On this basis it is judged that the conclusions of Reference 1 are applicable to the Millstone primary loops. Specifically, it can be concluded that a postulated []^{a,c,e} through-wall flaw in the Millstone loop piping will remain stable from both a local and global stability standpoint.

Actually for the Millstone loads and geometry, the applied J was estimated to be less than []^{a,c,e} which is significantly less than J_{MAX} for the []^{a,c,e}

A similar estimate was obtained for a []^{a,c,e} through-wall flaw. The purpose of the evaluation was to investigate the crack stability for a postulated flaw larger in size than the []^{a,c,e} reference flaw. For the Millstone Unit 3 maximum moment of []^{a,c,e} the maximum applied J was estimated to be []^{a,c,e}

The applied tearing modulus, T_{app}, was calculated using the methodology of Reference 1 and was less than []^{a,c,e} which is significantly less than T_{mat} for even the worst case []^{a,c,e} material of Reference 13. Therefore, it is further concluded that a postulated []^{a,c,e} through-wall flaw in the Millstone Unit 3 primary loop piping will remain stable from both a local and global stability standpoint.

TABLE 4-1 Chemical & Physical Properties of Millstone Unit No. 3
Primary Loop Material

4-6

a,c,e

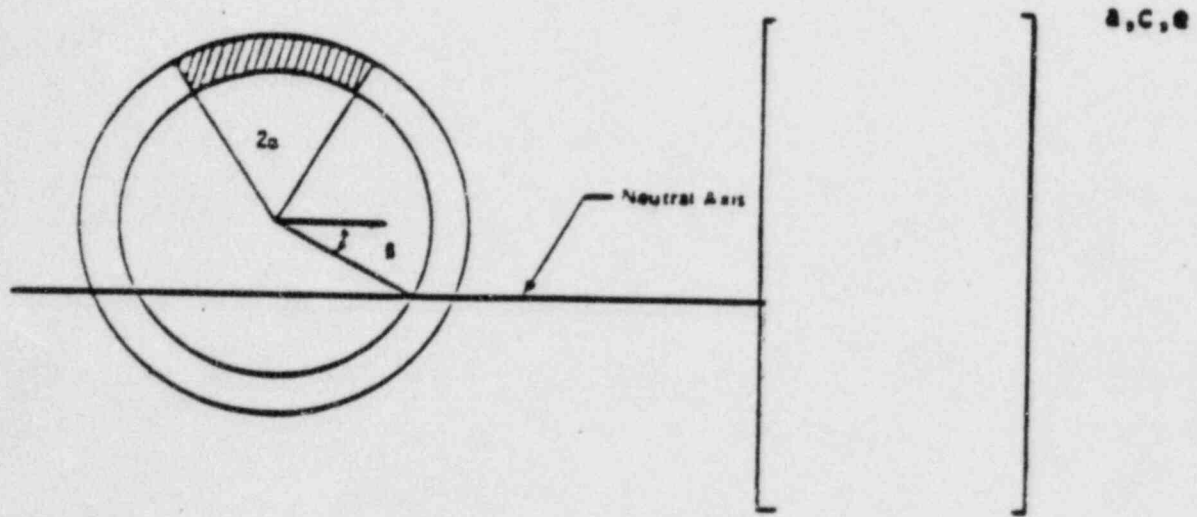


FIGURE 4-1 [a, c, e Stress Distribution]



FIGURE 4-2 J- Δa Curves at Different Temperatures. Aged Material []^{a,c,e}
(7500 Hours at 400°C)

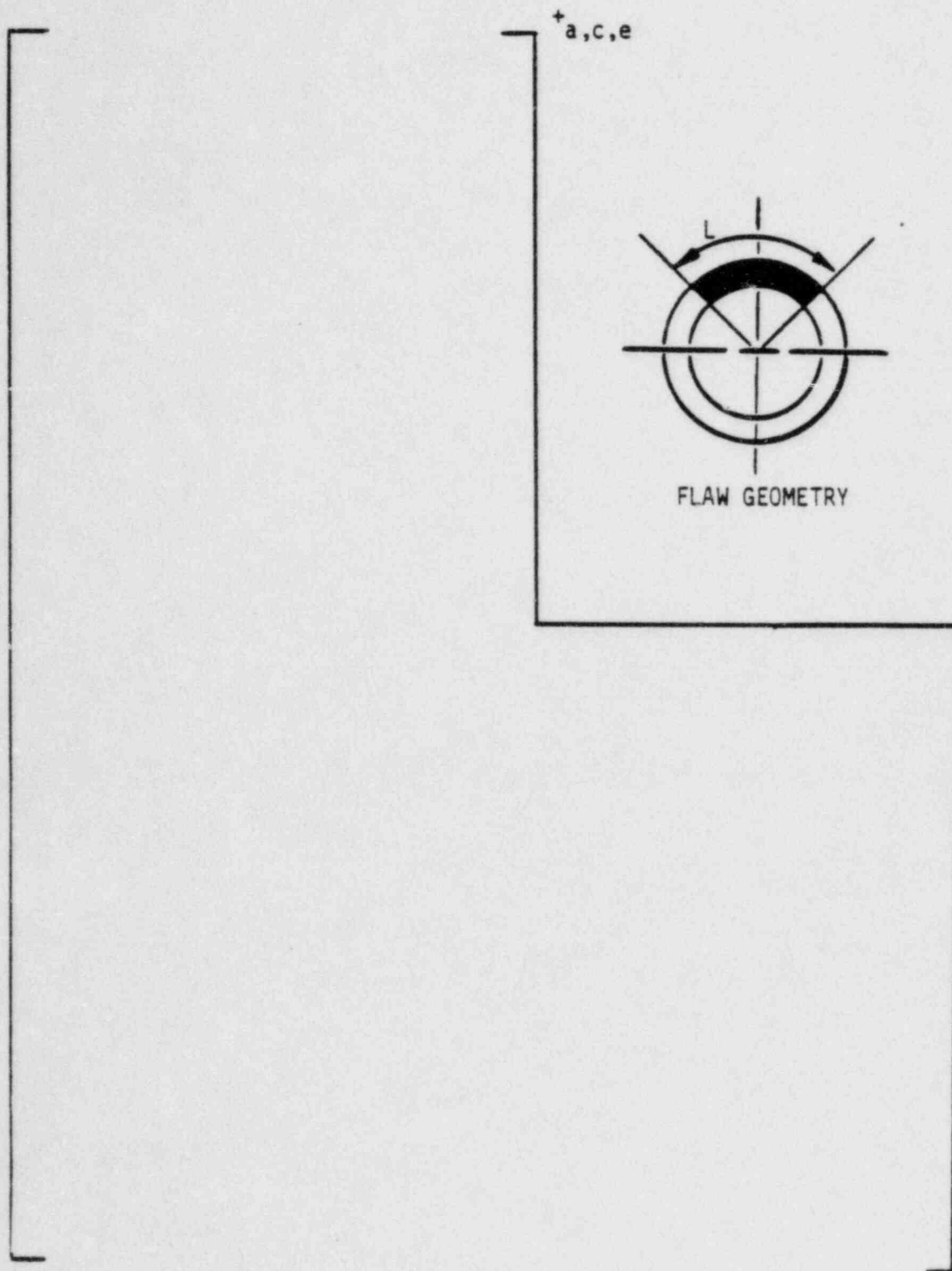


FIGURE 4-3 Critical Flaw Size Prediction

5.0 LEAK RATE PREDICTIONS

Leak rate estimates were performed by applying the normal operating bending moment of []^{a,c,e} in addition to the normal operating axial force of []^{a,c,e} to the hot leg pipe containing a postulated []^{a,c,e} through-wall flaw. The crack opening area was estimated using the method described in Reference 15. The leak rate was calculated using the two-phase flow formulation described in Reference 1. The computed leak rate was []^{a,c,e}. In order to determine the sensitivity of leak rate to flaw size, a through-wall flaw []^{a,c,e} in length was postulated. The calculated leak rate was []^{a,c,e}.

The Millstone Unit 3 plant has an RCS pressure boundary leak detection system which is consistent with the guidelines of Regulatory Guide 1.45 of detecting leakage of 1 gpm in one hour. Thus, for the []^{a,c,e} inch flaw, a factor in excess of []^{a,c,e} exists between the calculated leak rate and the criteria of Regulatory Guide 1.45. Relative to the []^{a,c,e}

6.0 FATIGUE CRACK GROWTH ANALYSIS

To determine the sensitivity of the primary coolant system to the presence of small cracks, a fatigue crack growth analysis was carried out for the []^{a,c,e} region of a typical system []

] ^{a,c,e} This region was selected because it is one of the important cross sections in the primary loop. Crack growth calculated here will be typical of that in the entire primary loop.

A [] ^{a,c,e} of a plant typical in geometry and operational characteristics to any Westinghouse PWR System. []

] ^{a,c,e}

All normal, upset, and test conditions were considered and circumferentially oriented surface flaws were postulated in the region, assuming the flaw was located in three different locations, as shown in Figure 6-1. Specifically, these were:

Cross Section A: [] ^{a,c,e}
Cross Section B: [] ^{a,c,e}
Cross Section C: [] ^{a,c,e}

Fatigue crack growth rate laws were used []

] ^{a,c,e} The law for stainless steel was derived from Reference 16, with a very conservative correction for the R ratio, which is the ratio of minimum to maximum stress during a transient. For stainless steel, the fatigue crack growth formula is:

$$\frac{da}{dn} = (5.4 \times 10^{-12}) K_{eff}^{4.48} \quad \text{inches/cycle}$$

where $K_{eff} = K_{max} (1-R)^{0.5}$

$$R = K_{min}/K_{max}$$

[

] a,c,e

[

]

a,c,e

where: [

] a,c,e

The calculated fatigue crack growth for semi-elliptic surface flaws of circumferential orientation and various depths is summarized in Table 6-1. The results show that the crack growth is very small, regardless [

] a,c,e

TABLE 6-1

FATIGUE CRACK GROWTH AT [

]a,c,e (40 YEARS)

INITIAL FLAW (IN)	FINAL FLAW (IN)		
	[] ^{a,c,e}	[] ^{a,c,e}	[] ^{a,c,e}
0.292	0.31097	0.30107	0.30698
0.300	0.31949	0.30953	0.31626
0.375	0.39940	0.38948	0.40763
0.425	0.45271	0.4435	0.47421

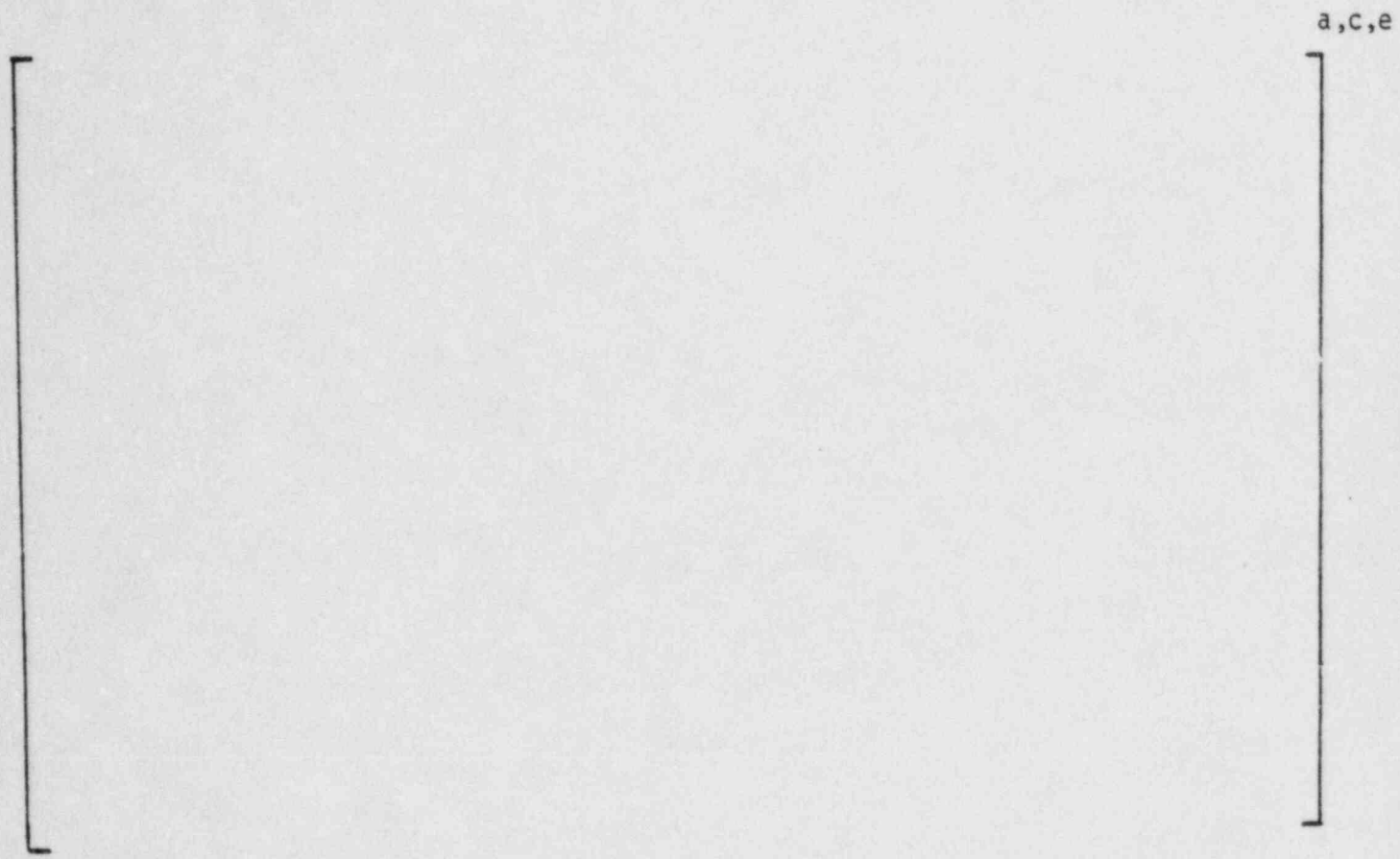


FIGURE 6-1 Typical Cross Section of []a,c,e

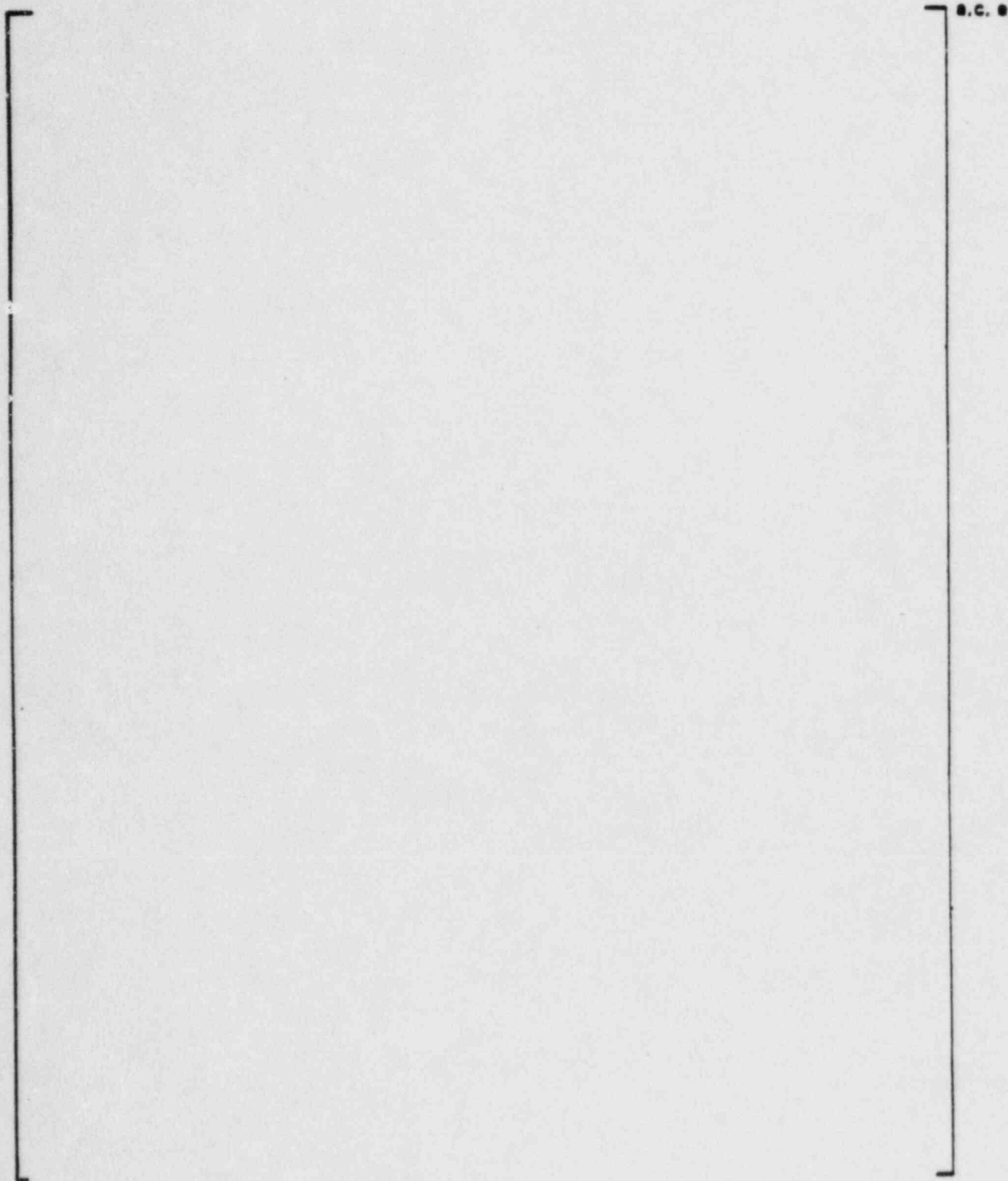


FIGURE 6-2 Reference Fatigue Crack Growth Curves For [a, c, e]

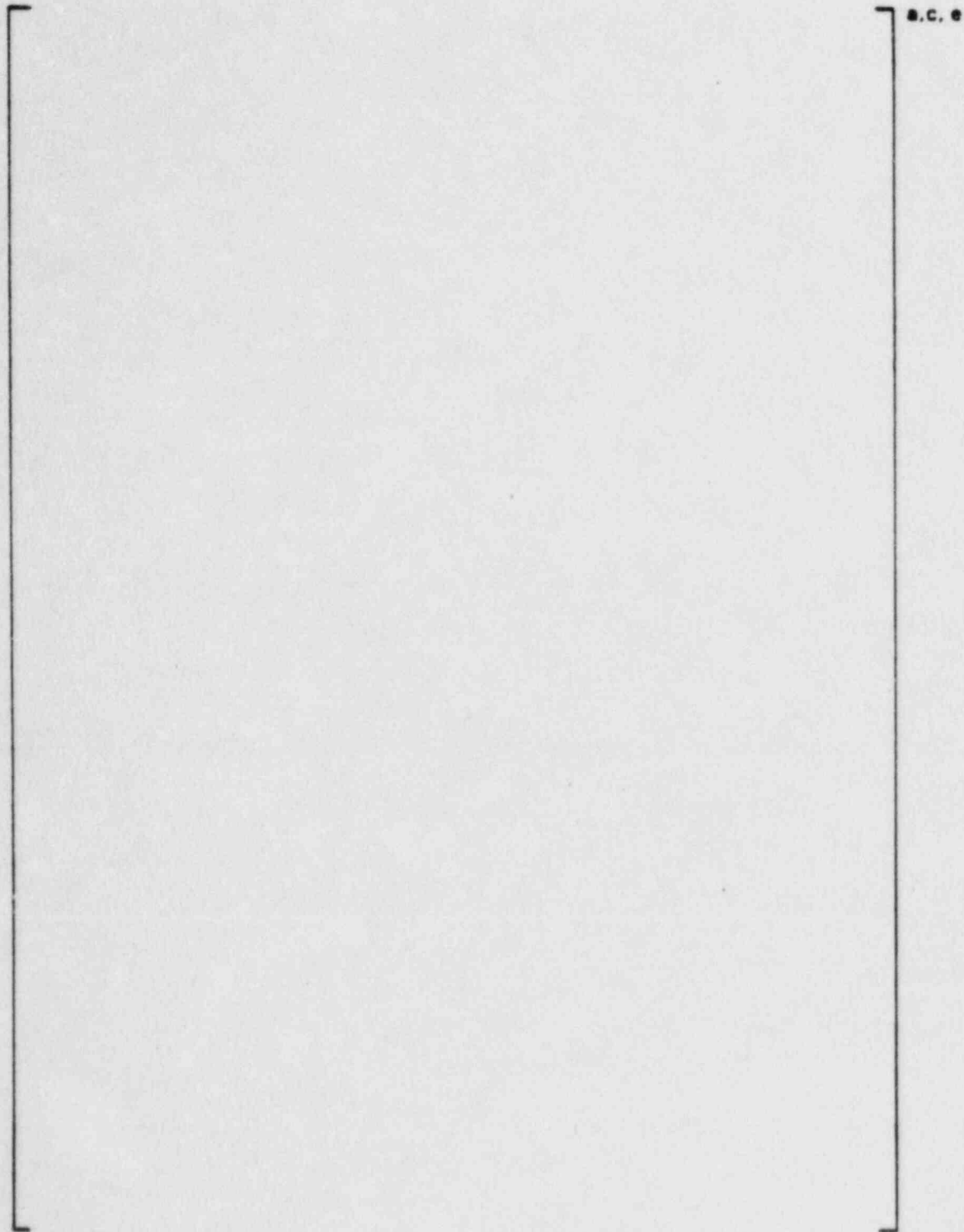


FIGURE 6-3 Reference Fatigue Crack Growth Law for [
in a Water Environment at 600°F

]a.c.e

7.0 ASSESSMENT OF MARGINS

In Reference 1, the maximum design moment was []^{a,c,e} whereas, the maximum moment as noted in Section 3.0 of this report is []^{a,c,e}. The maximum estimated value of J []^{a,c,e} as compared with the value of []^{a,c,e} in Reference 1. Furthermore, Section 4.3 shows the testing of fully aged material with chemistry more limiting than that existing in Millstone cast piping extended to J values of []^{a,c,e} which exceed the applied J value by 30 percent.

As shown in Section 3.0, margins of factors of greater than []^{a,c,e} and greater than []^{a,c,e} exist between calculated and ASME Code allowable faulted condition and thermal stresses, respectively.

Referring to Section 4.3, the estimated tearing modulus for Millstone Unit 3 cast stainless steel piping in the fully aged condition is at least []^{a,c,e} T_{app} for the reference flaw as taken from Reference 13 is []^{a,c,e} and is certainly less than the []^{a,c,e} calculated for the []^{a,c,e} flaw in Section 4.4. Consequently, a margin on local stability of at least []^{a,c,e} exists relative to tearing.

In Section 4.4, it is seen that a []^{a,c,e} flaw has a J value at maximum load of []^{a,c,e} which is also enveloped by the J_{max} of Reference 1 and the value used for testing of aged material. In Section 4.4, the critical flaw size using []^{a,c,e} methods is calculated to be []^{a,c,e}. Based on the above, the critical flaw size will, of course, exceed []^{a,c,e}.

In Section 5.0, it is shown that a flaw of []^{a,c,e} would yield a leak rate in excess of []^{a,c,e} while for a []^{a,c,e} flaw, the leak rate is []^{a,c,e}. Thus, there is a margin of at least []^{a,c,e} between the flaw size that gives a leak rate satisfying the criterion of Regulatory Guide 1.45 and the "critical" flaw size of []^{a,c,e}.

In summary, relative to

1. Loads

- a. Millstone Unit 3 is enveloped both by the maximum loads and J values in Reference 1 and the J values employed in testing of fully aged material.
- b. At the critical location, margins of []^{a,c,e} on faulted conditions and thermal stresses, respectively, exist relative to ASME Code allowable values.

2. Flaw Size

- a. A margin of at least []^{a,c,e} exists between the critical flaw and the flaw yielding a leak rate of []^{a,c,e}
- b. A margin exists of at least []^{a,c,e} relative to tearing.
- c. If []^{a,c,e} is used as the basis for critical flaw size, the margin for global stability would exceed []^{a,c,e} when compared to the reference flaw.

3. Leak Rate

A margin in excess of []^{a,c,e} exists for the reference flaw ([]^{a,c,e}) between calculated leak rates and the criteria of Regulatory Guide 1.45.

8.0 CONCLUSIONS

This report has established the applicability of the generic Westinghouse evaluations which justify the elimination of RCS primary loop pipe breaks for the Millstone plants as follows:

- a. The loads, material properties, transients, and geometry relative to the Millstone Unit 3 RCS primary loop are enveloped by the parameters of WCAP-9558, Revision 2 (Reference 1) and WCAP-10456 (Reference 13).
- b. Stress corrosion cracking is precluded by the use of fracture resistant materials in the piping system and controls on reactor coolant chemistry, temperature, pressure, and flow during normal operation.
- c. Water hammer should not occur in the RCS piping because of system design, testing, and operational considerations.
- d. The effects of low and high cycle fatigue on the integrity of the primary piping are negligible.
- e. A large margin exists between the leak rate of the reference flaw and the criteria of Reg. Guide 1.45.
- f. Ample margin exists between the reference flaw chosen for leak detectability and the critical flaw.
- g. Ample margin exists in the material properties used to demonstrate end-of-life (relative to aging) stability of the reference flaw.

The reference flaw will be stable throughout reactor life because of the ample margins in e, f, and g above and will leak at a detectable rate which will assure a safe plant shutdown.

Based on the above, it is concluded that RCS primary loop pipe breaks should not be considered in the structural design basis for Millstone Unit 3.

9.0 REFERENCES

1. WCAP-9558, Rev. 2, "Mechanistic Fracture Evaluation of Reactor Coolant Pipe Containing a Postulated Circumferential Through-Wall Crack," Westinghouse Proprietary Class 2, June 1981.
2. USNRC Generic letter 84-04, Subject: "Safety Evaluation of Westinghouse Topical Reports Dealing with Elimination of Postulated Pipe Breaks in PWR Primary Main Loops", February 1, 1984.
3. WCAP-8082 P-A, "Pipe Breaks for the LOCA Analysis of the Westinghouse Primary Coolant Loop," Class 2, January 1975.
4. Letter from Westinghouse (E. P. Rahe) to NRC (R. H. Vollmer), NS-EPR-2768, dated May 11, 1983.
5. WCAP-9283, "The Integrity of Primary Piping Systems of Westinghouse Nuclear Power Plants During Postulated Seismic Events," March, 1978.
6. WCAP-9787, "Tensile and Toughness Properties of Primary Piping Weld Metal for Use in Mechanistic Fracture Evaluation", Westinghouse Proprietary Class 2, May 1981.
7. Letter Report NS-EPR-2519, Westinghouse (E. P. Rahe) to NRC (D. G. Eisenhut), Westinghouse Proprietary Class 2, November 10, 1981.
8. Letter from Westinghouse (E. P. Rahe) to NRC (W. V. Johnston) dated April 25, 1983.
9. Letter from Westinghouse (E. P. Rahe) to NRC (W. V. Johnston) dated July 25, 1983.
10. NUREG-0691, "Investigation and Evaluation of Cracking Incidents in Piping in Pressurized Water Reactors", USNRC, September 1980.

11. Kanninen, M. F., et. al., "Mechanical Fracture Predictions for Sensitized Stainless Steel Piping with Circumferential Cracks", EPRI NP-192, September 1976.
12. Bush, A. J., Stouffer, R. B., "Fracture Toughness of Cast 316 SS Piping Material Heat No. 156576, at 600°F", Westinghouse R D Memo No. 83-5P6EVMTL-M1, Westinghouse Proprietary Class 2, March 7, 1983.
13. WCAP-10456, "The Effects of Thermal Aging on the Structural Integrity of Cast Stainless Steel Piping For Westinghouse NSSS," Westinghouse Proprietary Class 2, November 1983.
14. Slama, G., Petrequin, P., Masson, S. H., and Mager, T. R., "Effect of Aging on Mechanical Properties of Austenitic Stainless Steel Casting and Welds", presented at SMIRT-7 Post Conference Seminar 6 - Assuring Structural Integrity of Steel Reactor Pressure Boundary Components, August 29/30, 1983, Monterey, CA.
15. NUREG/CR-3464, "The Application of Fracture Proof Design Methods using Tearing Instability Theory to Nuclear Piping Postulating Circumferential Through Wall Cracks" 1983.
16. Bamford, w. H., "Fatigue Crack Growth of Stainless Steel Piping in a Pressurized Water Reactor Environment", Trans. ASME Journal of Pressure Vessel Technology, Vol. 101, Feb. 1979.

- | | | | |
|-----|---|---|-------|
| 17. | [|] | a,c,e |
| 18. | [|] | a,c,e |

APPENDIX A

a,c,e

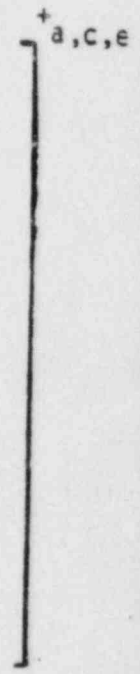
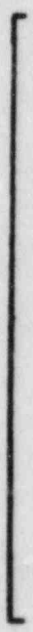


FIGURE A-1 Pipe with a through-wall crack in bending